RESEARCH ARTICLE | MAY 12 2022

Supercritical CO_2 mixtures for Brayton power cycles complex configurations with concentrating solar power

Robert Valencia-Chapi ✉; Paul Tafur-Escanta; Luis Coco-Enríquez; Javier Muñoz-Antón

AIP Conf. Proc. 2445, 090009 (2022)
https://doi.org/10.1063/5.0086032

Supercritical CO_2 Mixtures for Brayton Power Cycles Complex Configurations with Concentrating Solar Power

Robert Valencia-Chapi[1,2,3,a)], Paul Tafur-Escanta[1], Luis Coco-Enríquez[1,4], Javier Muñoz-Antón[1]

[1] *Universidad Politécnica de Madrid. C/ José Gutiérrez Abascal, 2. 28006, Madrid, Spain*
[2] *Investigación, Desarrollo e Innovación energética, S.L. C/ Oria, 16. 28002 Madrid, Spain*
[3] *Universidad Técnica del Norte. Av. 17 de Julio, 5-21. 100105, Ibarra, Ecuador*
[4] *Universidad Internacional de la Rioja. Av. de la Paz, 137. 26006, Logroño, Spain*

[a)] Corresponding author: robert.valencia.chapi@upm.es

Abstract. An evaluation of the impact of using supercritical carbon dioxide mixtures (s-CO_2/C_2H_6, s-CO_2/CH_4, s-CO_2/Kr, and s-CO_2/SF_6) as a working fluid is made here for Brayton s-CO_2 power cycles. The considered complex configurations include recompression with two reheating (RCC–2RH), recompression with three reheating (RCC–3RH), recompression with main compressor intercooling and two reheating (RCMCI–2RH), and recompression with main compressor intercooling and three reheating (RCMCI–3RH), which were coupled to a linear-focus solar system with Solar Salt (60% $NaNO_3$/40% KNO_3) as the heat transfer fluid (HTF). The design parameters evaluated the solar plant performance at the design point, the aperture area of the solar field, and variations in costs regarding the plant's total conductance (UA_{total}). The methodology used to calculate the performance established the total conductance values of the heat recuperator (UA_{total}) to between 5 and 25 MW/K. The main conclusion is that the cycle efficiency has a considerable improvement compared with that obtained using pure s-CO_2. The s-CO_2/Kr mixture with a molar fraction ratio of 30/70 increases the cycle efficiency between 7–11% relative to pure s-CO_2 and as a function of the UA_{total}. The s-CO_2/CH_4 mixture with a molar fraction of 45/55 increases between 3–7%, and the s-CO_2/C_2H_6 and s-CO_2/SF_6 mixtures only increase between 1–2%. For the solar field unitary costs, the s-CO_2/Kr mixture has the lowest cost at $29–34 million USD, which depends on the solar field aperture area and the UA_{total} for the RCC-2RH and RCMCI-2RH configurations. Finally, the results demonstrate that variations in the working fluid properties play a significant role due to the positive impact on the increased thermal efficiency of the s-CO_2 Brayton cycle when using the RCC and RCMCI configurations.

INTRODUCTION

Supercritical carbon dioxide (s-CO_2) power cycles are widely regarded as one of the promising alternative energy conversion systems for next-generation concentrating solar power (CSP) technologies (CSP Gen3) [1]. The need to improve efficiencies and have a working fluid that adapts to variable environments in power plants highlights the importance of optimizing equipment designs and the inlet and operating conditions [2]. These factors have focused research on the emergence of combining different s-CO_2 power cycle configurations with CSP technologies in terms of costs and thermal efficiency. Thus, it is crucial to consider mixtures with s-CO_2 as the working fluid to analyze their effects on the operating conditions, mainly the efficiency [3,4].

Various s-CO_2 Brayton cycle configurations are currently being studied [5–8]. Al-Sulaiman et al. [9] determined that the recompression cycle has the best performance compared to other configurations as it is simple and exhibits pre-compression and split expansion. Marchionni et al. [6] analyzed eight s-CO_2 power cycle designs by varying the turbine inlet temperature (TIT) to between 250 and 600 °C. The analysis shows that more complex Brayton s-CO_2 cycles lead to a higher overall efficiency and net power output with higher investment costs. Neises et al. [7] studied the design, performance, and cost of simple recompression and partial cooling configurations in s-CO_2 power cycles coupled with a Solar Tower, which uses molten salt as a heat transfer fluid (HTH). Linares et al. [8] proposed four

SolarPACES 2020
AIP Conf. Proc. 2445, 090009-1–090009-9; https://doi.org/10.1063/5.0086032
Published by AIP Publishing. 978-0-7354-4195-8/$30.00

new configurations and studied four specific designs of a Brayton s-CO_2 cycle with recompression for central-tower solar plants. In the two considered scenarios of dry and wet cooling, the plant first achieves the highest efficiency in recompression for a cooling and reheating design with a 52.6% efficiency at a 300 bar turbine inlet pressure. In the wet-cooling scenario, the non-intercooled, non-superheated recompression cycle exceeded a 51% efficiency at 250 bars, increasing to more than 54% if superheat is added. Finally, Valencia et al. [2] studied the influence of fluid mixtures on a Brayton s-CO_2 cycle with recompression, and showed that the mixtures increase the cycle efficiency by 3–4%.

The primary purpose of this study is to compare the benefits of s-CO_2 mixtures (s-CO_2/C_2H_6, s-CO_2/CH_4, s-CO_2/Kr, and s-CO_2/SF_6) in complex s-CO_2 Brayton power cycle configurations (Figures 1 and 2) coupled to a CSP plant with parabolic trough collector (PTC) technology.

MATERIALS AND METHODS

A constant total heat recuperator conductance (UA_{total}) was set to calculate the plant performance [10]. Some complex Brayton cycle configurations that have been studied are the recompression with two reheating (RCC–2RH), recompression with three reheating (RCC–3RH), recompression with main compressor intercooling and two reheating (RCMCI–2RH), and recompression with main compressor intercooling and three reheating (RCMCI–3RH). The Supercritical Concentrated Solar Power Plant (SCSP) software [11] has been used to simulate the performance of complex configurations at the design-point (Figs. 1 and 2) when operating with a power cycle working fluid of pure s-CO_2 and s-CO_2 mixtures. The fluid properties (Fig. 3) were obtained from the REFPROP database as developed by NIST in the USA [12]. The main assumptions considered are summarized in Table 1.

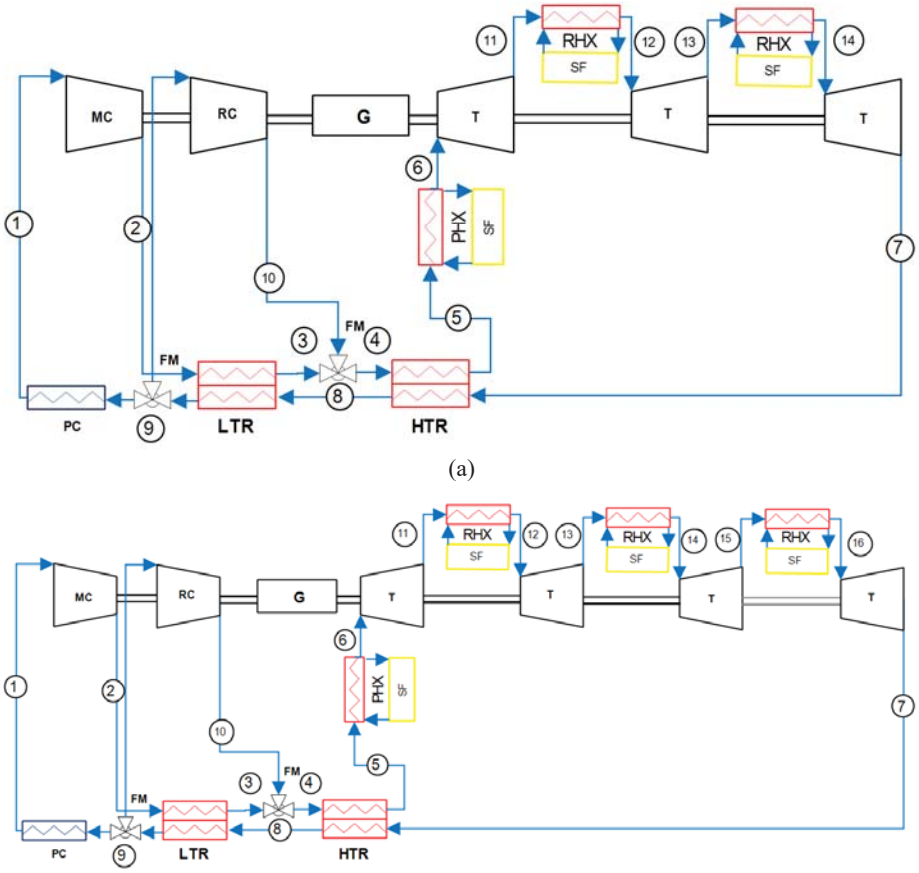

FIGURE 1. Recompression Brayton cycle with two reheating (a) and three reheating (b) layouts. MC: main compressor; RC: recompressor; G: generator; T: turbine; PC: precooler; FS: fluid split; FM: fluid mixture; LTR: low-temperature recuperator; HTR: high-temperature recuperator; PHX: primary heat exchanger; RHX: reheating heat exchanger; SF: solar field

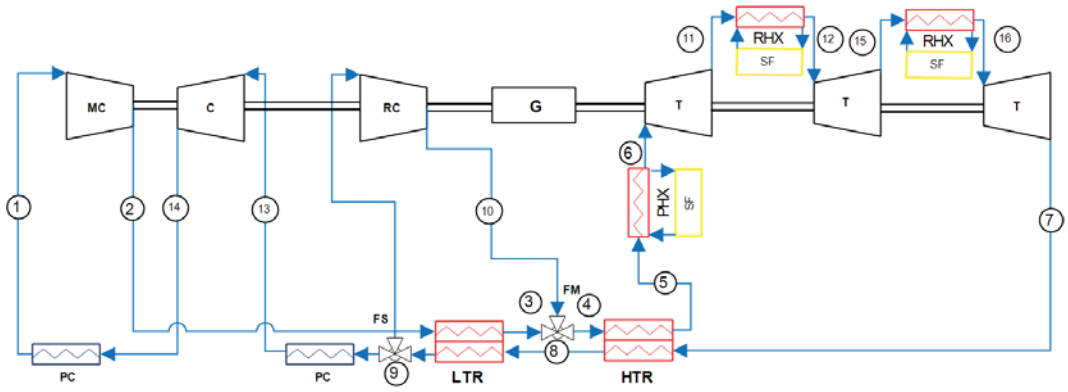

(a)

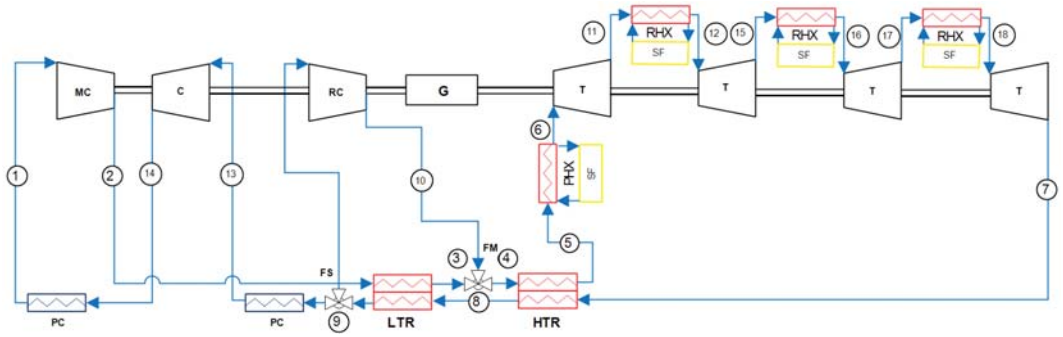

(b)

FIGURE 2. Recompression with main compressor intercooling Brayton cycle with two reheating (a) and three reheating (b) layouts. MC: main compressor; RC: recompressor; C: compressor; G: generator; T: turbine; PC: precooler; FS: fluid split; FM: fluid mixture; LTR: low-temperature recuperator; HTR: high-temperature recuperator; PHX: primary heat exchanger; RHX: reheating heat exchanger; SF: solar field

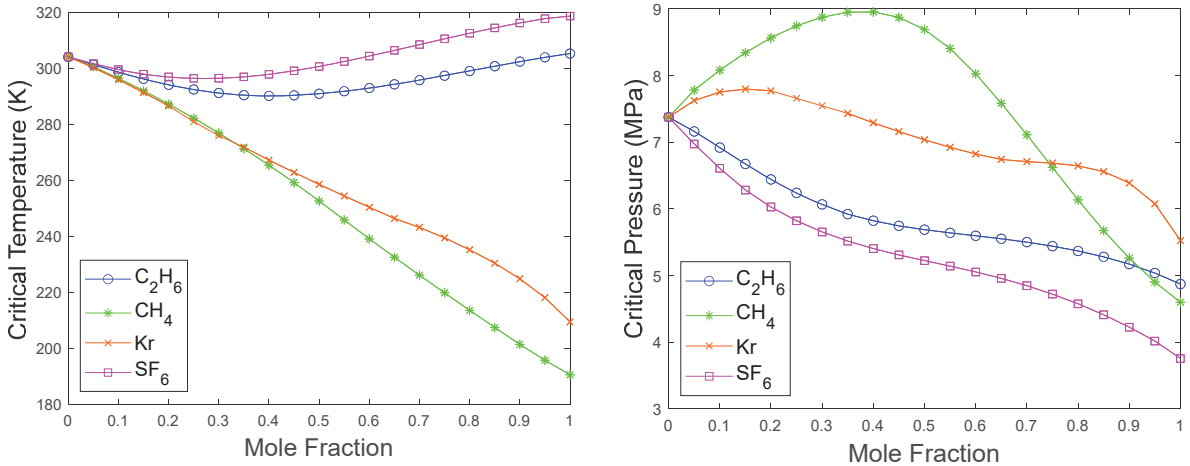

(a) (b)

FIGURE 3. Fluid properties: (a) critical temperature vs mole fraction, and (b) critical pressure vs mole fraction

TABLE 1. Input parameters for mixtures that decrease the critical temperature.

Assumptions	Nomenclature	Value	Units
Net power output	W	50	MW
Compressor inlet temperature	T_1	Optimized	ºC
Compressor inlet pressure	P_1	Optimized	MPa
Turbine inlet temperature	T_6	550	ºC
Turbine inlet pressure	P_6	25	MPa
Compressor efficiency [2]	η_{mc}	0.89	-
Turbine efficiency [2]	η_t	0.93	-
Heat exchanger conductance for the low-temperature recuperator [2,11]	UA_{LT}	2.5 → 12.5	MW/K
Heat exchanger conductance for the high-temperature recuperator [2,11]	UA_{HT}	2.5 → 12.5	MW/K
Split fraction	γ	Optimized	-

The boundaries considered for optimization in terms of the temperature and pressure always operate with values above the fluid critical values. The results show that the cycle thermal efficiency is maximized when the CIT is slightly above the critical temperature, as shown in Tables 2 and 3. The efficiency of these cycles compared to their recuperator total conductance using pure s-CO_2 as the working fluid and without pressure drop in the components is shown in Fig. 4.

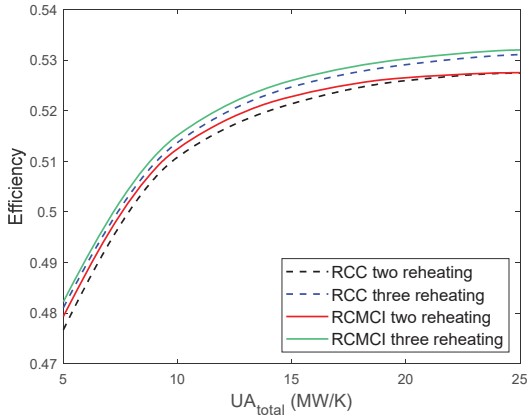

FIGURE 4. Cycle efficiency vs UA_{total} with the RCC having two and three reheating, and the RCMCI having two and three reheating Brayton cycles using pure s-CO_2.

RESULTS AND DISCUSSION

The plant's gross efficiency is calculated by setting the total recuperator conductance (UA_{total}) for a given TIT. The reheating pressure, compressor inlet pressure, compressor inlet temperature, and split fraction are optimized with the SUBPLEX [15], NEWOUA [16], and BOBYQA [17] algorithms. As shown in Tables 2 and 3, the optimal efficiency in most cases is obtained when the mixture's critical temperature (CIT opt.) is close to or a few units above the compressor inlet temperature (CIT crit.). The mixture s-CO_2/SF_6 (90/10) in the power cycle configurations for the recompression with a main compressor intercooling and two and three reheating have the most significant variations compared to the critical CIT. In the RCC–2RH configuration, the optimal efficiency is ten units above the critical CIT, while in the RCMCI–2RH and RCMCI–3RH configurations, the optimal efficiency is five units above the critical CIT. The optimal mixing efficiency for the s-CO_2/Krypton (30/70) mixture in the RCMCI – 3RH configuration is seven units above the critical CIT when the UA_{total} is valued at 30 MW/K.

The working fluid density is a constraint factor in the power cycle equipment dimensions. If the density increases, the compressor and turbine sizes are minimized. When krypton is used in the s-CO_2/Kr (30/70) mixture, it has a higher density at approximately 878.04 kg/m^3. Figures 5 and 7 in the RCC with two and three reheating suggest that mixtures with decreasing critical temperatures produce an increased efficiency over cycles of pure s-CO_2. Table 2 shows the properties of the mixtures used in the RCC configurations. The property calculations are performed under optimized temperature and pressure conditions; that is, those that maximize the efficiency.

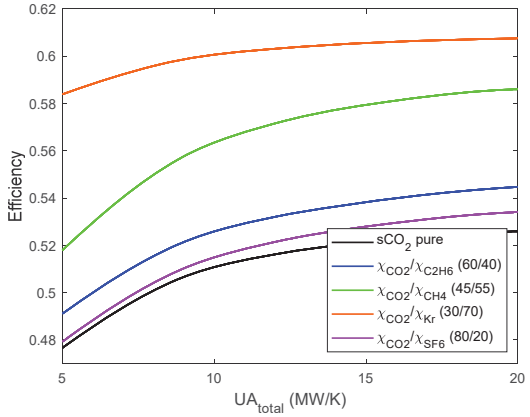

FIGURE 5. Cycle efficiency vs. UA_{total} the RCC having two reheating Brayton cycles using s-CO_2 mixtures

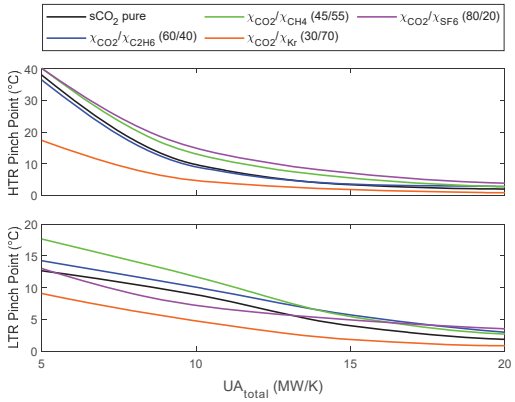

FIGURE 6. LTR and HTR pinch point vs. UA_{total} with the RCC having two reheating Brayton cycles using s-CO_2 mixtures

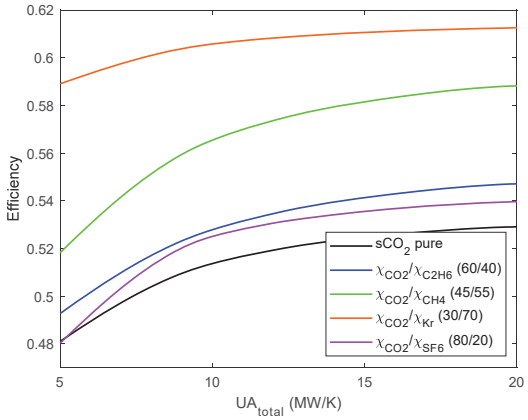

FIGURE 7. Cycle efficiency vs UA_{total} with the RCC having three reheating Brayton cycles using s-CO_2 mixtures

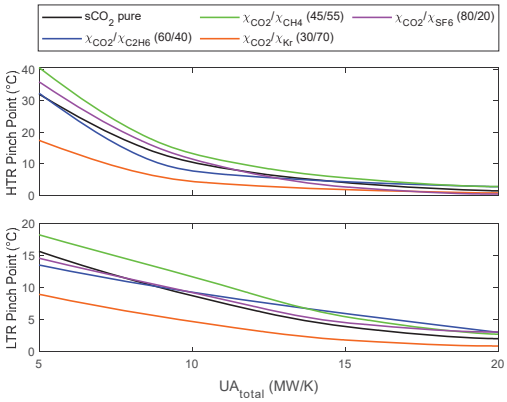

FIGURE 8. LTR and HTR pinch point vs UA_{total} with the RCC having three reheating Brayton cycles using s-CO_2 mixtures

TABLE 2. Results and thermophysical properties of mixtures in RCC configurations

Mixtures	CIT Crit. (K)	CIT Opt. (K)	CIP (Opt.) (MPa)	Density (kg/m^3)	Cp (kJ/kg K)	Thermal conductivity (W/m K)	Kinematic viscosity (cm^2/s)	Prandtl	η_{th}
s.CO_2 pure	304.1	304.1	7.37	467.6	107570	2.3956	6.9E-04	1452.7	0.5214
s-CO_2 / C_2H_6 (60/40)	290.2	291.2	5.89	251.71	28.21	6.91E-01	8.35E-04	8.5302	0.5447
s-CO_2 / CH_4 (45/55)	245.9	246.0	8.41	365.44	6.2678	6.76E-02	7.87E-04	2.6659	0.5860
s-CO_2 / Kr (30/70)	243.2	243.3	6.93	982.23	5.1567	4.39E-02	5.25E-04	6.0552	0.6075
s-CO_2 / SF_6 (80/20)	296.9	306.9	6.029	266.85	2.2038	3.00E-02	7.97E-04	1.5485	0.5341

Figures 9 and 11 in the RCMCI with two and three reheating suggest that mixtures with decreasing critical temperatures produce an increased efficiency over cycles of pure s-CO_2. The total recuperator conductance (UA_{total}) is related to the increased cycle efficiency. This increase is limited by decreases in the "pinch point," which is defined as the minimum difference in temperature between each heat recovery unit (LTR and HTR). Figures 6 and 8 for the RCC configurations and Figs. 10 and 12 for the RCMCI configurations show that increasing the UA_{total} decreases the pinch point.

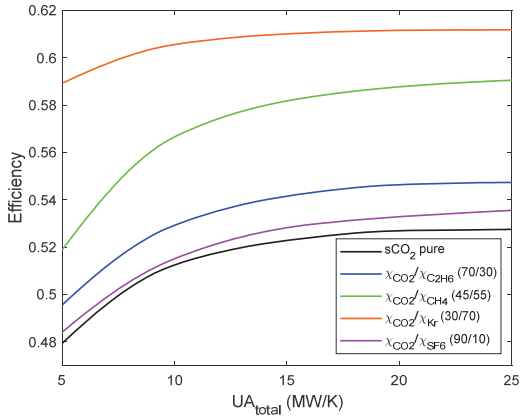

FIGURE 9. Cycle efficiency vs UA_{total} with the RCMCI having two reheating Brayton cycles using s-CO_2 mixtures

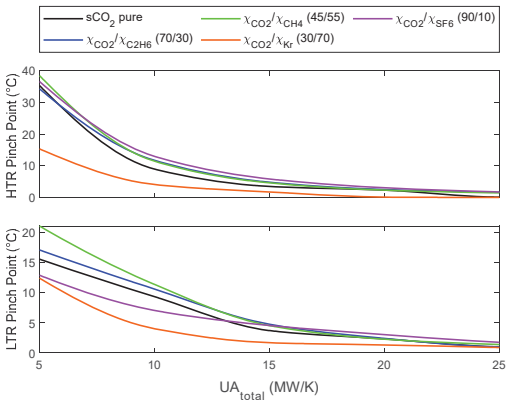

FIGURE 10. LTR and HTR pinch point vs UA_{total} with the RCMCI having two reheating Brayton cycles using s-CO_2 mixtures

The results show that the efficiency follows a constant trend when the UA_{total} exceeds 20 MW/K for the RCMCI configurations with Brayton s-CO_2 power cycles using the s-CO_2/Kr and s-CO_2/C_2H_6 mixtures whose molar fractions are 30/70 and 70/30, respectively. Table 3 shows the properties of the mixtures used under the RCMCI configurations. The property calculations are performed with the optimized temperature and pressure conditions; that is, those that maximize efficiency.

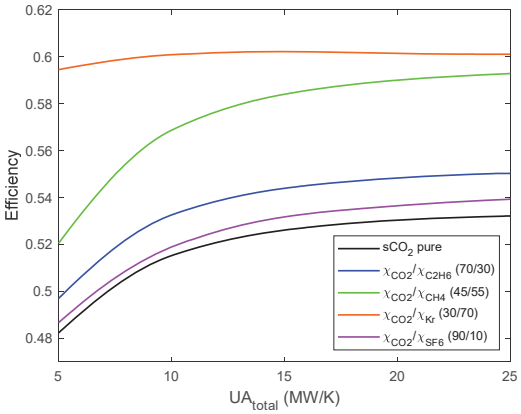

FIGURE 11. Cycle efficiency vs UA_{total} with the RCMCI having three reheating Brayton cycles using s-CO_2 mixtures

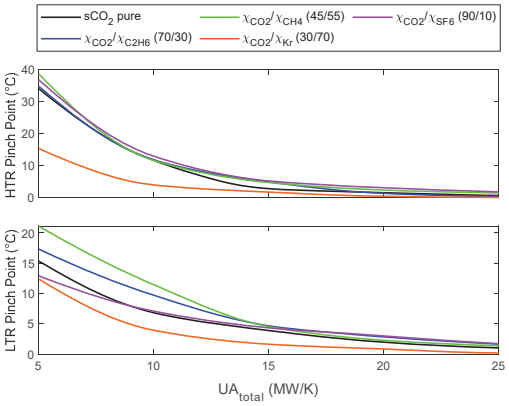

FIGURE 12. LTR and HTR pinch point vs UA_{total} with the RCMCI having three reheating Brayton cycles using s-CO_2 mixtures

TABLE 3. Results and thermophysical properties of mixtures under the RCMCI configurations

Mixtures	CIT Crit. (K)	CIT Opt. (K)	CIP (Opt.) (MPa)	Density (kg/m^3)	Cp (kJ/kg K)	Thermal conductivity (W/m K)	Kinematic viscosity (cm^2/s)	Prandtl	η_{th}
s-CO_2 pure	304.1	304.1	7.37	467.6	107570	2.3956	6.9E-04	1452.7	0.5320
s-CO_2 / C_2H_6 (70/30)	290.2	294.2	6.07	208.80	6.6846	4.38E-01	8.88E-04	2.8292	0.5445
s-CO_2 / CH_4 (45/55)	245.9	246.0	8.41	365.44	6.2678	6.76E-02	7.87E-04	2.6659	0.5921
s-CO_2 / Kr (30/70)	243.2	243.3	6.725	880.96	6.3035	4.25E-02	5.09E-04	6.6316	0.6118
s-CO_2 / SF_6 (90/10)	299.6	304.6	6.61	278.06	3.7329	3.72E-02	7.78E-04	2.1671	0.5389

The total recuperator conductance is directly related to the increased cycle efficiency. This increase is limited by the decreased pinch point, which is defined as the minimum temperature difference between the hot and cold streams in each heat recuperator (LTR and HTR). The recuperator characteristic operating values are considered pinch point temperatures between 5–10 °C; however, these temperatures can be reduced to a range of 1–5 °C in the studied configurations [11].

Estimating the cost of a CSP plant becomes complicated when considering the level of detail required. The main problem is the lack of data, especially with relatively new technologies such as the Brayton s-CO_2 power cycle. Therefore, cost estimates are made here for the solar field's parabolic trough collectors (SF-PTC). The estimated cost of the solar field is given by the equation:

$$SF_{Cost} = SF_{EA} * C_{UC} * CF \tag{1}$$

where SF_{Cost} is the cost of the solar field, SF_{EA} is the effective area of the solar field, C_{UC} is the unit cost of the collector, and CF is the construction factor of the solar field. The cost values are shown in Table 4 [11]. The SF-PTC costs are compared to the cycle total recuperator conductance. The solar field cost decreases when the UA_{total} increases, as seen in Figs. 13 and 14. The s-CO_2/Kr (30/70) mixture implies a lower cost for the considered configurations. Figure 15 shows that the heat exchanger pressure drop negatively impacts the cycle thermal efficiency. Therefore, the research community has focused on studying and designing heat exchangers used in Brayton cycles.

TABLE 4. Unit costs of the PTC with molten salts as the HTF

	Value	Units
PTC with AISI 347 Solar Salt as HTF	432	$/m^2
Construction factor	1.16	-

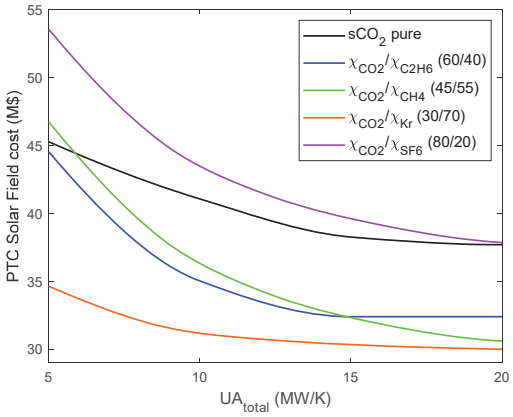

FIGURE 13. PTC solar field cost vs UA_{total} with the RCC-2RH Brayton cycle using s-CO_2 mixtures

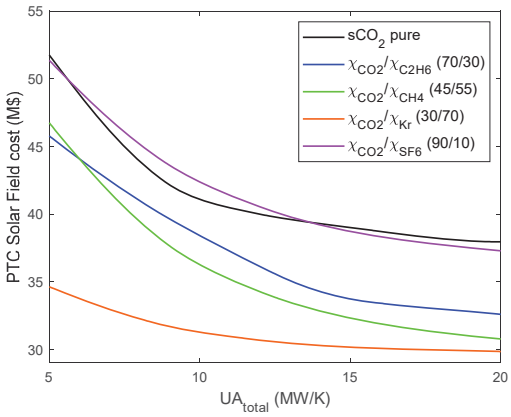

FIGURE 14. PTC solar field cost vs UA_{total} with the RCMCI-2RH Brayton cycle using s-CO_2 mixtures

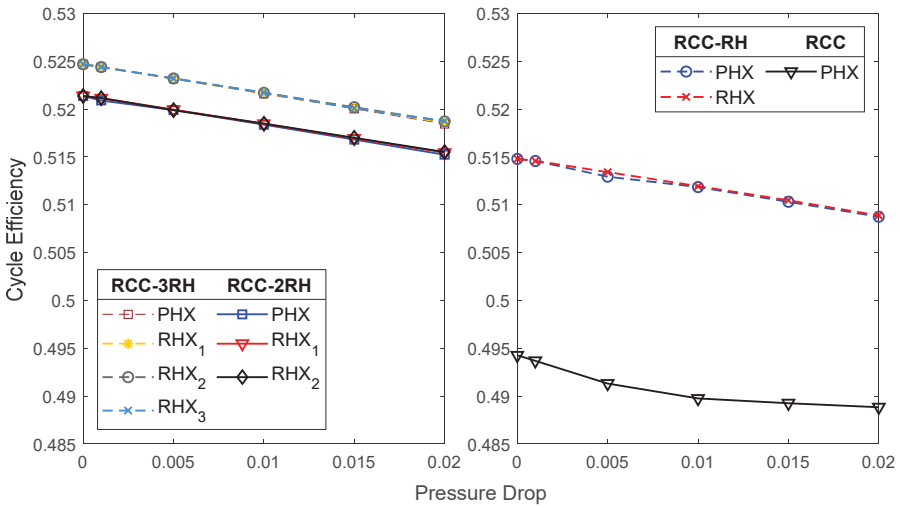

FIGURE 15. Cycle efficiency vs pressure drop with the RCC, RCC-RH, RCC-2RH, and RCC-3RH Brayton cycles using pure s-CO_2 with UA_{total} = 15 MW/K

CONCLUSIONS

The main conclusion of this work is that the s-CO_2 mixture directly impacts the thermal efficiency of Brayton power cycles, as previously proposed [2–4]. This study shows the need to investigate supercritical fluid mixtures as working fluids in different Brayton power cycles. Mixtures with ethane s-CO_2/C_2H_6 (60/40) for the RCC configurations and s-CO_2/C_2H_6 (70/30) for the RCMCI configurations increase the cycle efficiency from 49% to 55% as a function of the total conductance of the heat reheaters. The s-CO_2/CH_4 (45/55) mixture tends to increase the cycle efficiency from 51% to 58% for the RCC cycles and 52% to 59% for the RCMCI cycles. The s-CO_2/Kr (30/70) mixture increases the efficiency from 58% to 60% (RCC-2RH), from 59% to 61% (RCC-3RH and RCMCI-2RH), and from 59% to 60% (RCMCI-3RH). Furthermore, as an inert gas mixed with carbon dioxide, krypton is a beneficial fluid as it could avoid corrosion problems in equipment materials. The s-CO_2/SF_6 (80/20) mixture improves the cycle efficiency from 47% to 53% for the RCC cycle, and the same mixture with a molar fraction (90/10) improves from 48% to 54% for the other three cycle configurations. Comparing the solar field costs obtained with the s-CO_2 mixtures, it is inferred that krypton mixtures produce the least cost because the cycle operates with a smaller opening area of the PTC. Its costs are between $29 and 34 million USD, depending on the UA_{total} and the power cycle configuration. Future work must consider pressure drops in the cycle components, especially in the recuperators and heat exchangers, to evaluate real improvements.

NOMENCLATURE

C_2H_6	Ethane	RCC-RH	Recompression with Reheating
CH_4	Methane	RCMCI	Recompression with Main Compressor Intercooling
CIP	Compressor Inlet Pressure	RCMCI-2RH	Recompression with Main Compressor Intercooling and Two Reheating
CIT	Compressor Inlet Temperature	RCMC-3RH	Recompression with Main Compressor Intercooling and Three Reheating
CSP	Concentrating Solar Power	REFPROP	Reference Fluid Properties
Kr	Krypton	SF_6	Sulfur Hexafluoride
PTC	Parabolic Trough Solar Collector	s-CO_2	Supercritical Carbon Dioxide
RCC	Recompression	SCSP	Supercritical Concentrating Solar Power Plant

RCC-2RH	Recompression with Two Reheating	TIT	Turbine Inlet Temperature
RCC-3RH	Recompression with Three Reheating	UA	Conductance: heat exchanger product of overall heat transfer coefficient (U) and heat, transfer surface (A)

REFERENCES

1. Yin JM, Zheng QY, Peng ZR, Zhang XR. Review of supercritical CO_2 power cycles integrated with CSP. Int J Energy Res. 2020;44(3):1337–69. Available from: https://onlinelibrary.wiley.com/doi/abs/10.1002/er.4909
2. Valencia-Chapi R, Coco-Enríquez L, Muñoz-Antón J. Supercritical CO_2 Mixtures for Advanced Brayton Power Cycles in Line-Focusing Solar Power Plants. Appl Sci. 2019; Available from: https://doi.org/10.3390/app10010055
3. Vesely L. Thesis: Study of Power Cycle with Supercritical CO_2. Czech Technical University in Prague; 2018. Available from: https://pdfs.semanticscholar.org/4914/4a496e3456eb45e0ea5cc2f07bffa2964f4e.pdf?_ga=2.199714603.422084581.1576280964-1144149164.1576280964
4. Manzolini G, Binotti M, Bonalumi D, Invernizzi C, Iora P. CO_2 Mixtures as Innovative Working Fluid in Power Cycles Applied to Solar Plants. Techno-Economic Assessment. Sol Energy. 2019; Available from: https://doi.org/10.1016/j.solener.2019.01.015
5. Crespi F, Gavagnin G, Sánchez D, Martínez GS. Supercritical Carbon Dioxide Cycles for Power Generation: A Review. Appl Energy. 2017;195:152–83. Available from: http://dx.doi.org/10.1016/j.apenergy.2017.02.048
6. Marchionni M, Bianchi G, Tassou SA. Techno-Economic Assessment of Joule-Brayton Cycle Architectures for Heat to Power Conversion from High-Grade Heat Sources Using CO_2 in the Supercritical State. Energy. 2018;148:1140–52. Available from: https://doi.org/10.1016/j.energy.2018.02.005
7. Neises T, Turchi C. Supercritical Carbon Dioxide Power Cycle Design and Configuration Optimization to Minimize Levelized Cost of Energy of Molten Salt Power Towers Operating at 650 °C. Sol Energy. 2019;181(January):27–36. Available from: https://doi.org/10.1016/j.solener.2019.01.078
8. Linares JI, Montes MJ, Cantizano A, Sánchez C. A novel supercritical CO_2 recompression Brayton power cycle for power tower concentrating solar plants. Appl Energy. 2020;263(April):114644. Available from: https://doi.org/10.1016/j.apenergy.2020.114644
9. Al-Sulaiman FA, Atif M. Performance Comparison of Different Supercritical Carbon Dioxide Brayton Cycles Integrated with a Solar Power Tower. Energy. 2015;82:61–71. Available from: http://dx.doi.org/10.1016/j.energy.2014.12.070
10. Dyreby JJ. Thesis: Modeling the Supercritical Carbon Dioxide Brayton Cycle with Recompression. University of Wisconsin-Madison; 2014. Available from: https://sel.me.wisc.edu/publications/theses/dyreby14.zip
11. Coco-Enríquez L. Thesis: Nueva Generación de Centrales Termosolares con Colectores Solares Lineales Acoplados a Ciclos Supercriticos de Potencia. Universidad Politécnica de Madrid; 2017. Available from: https://doi.org/10.20868/UPM.thesis.44002
12. Lemmon EW, Bell IH, Huber ML, McLinden MO. NIST Standard Reference Database 23: Reference Fluid Thermodynamic and Transport Properties-REFPROP, Version 10.0. National Institute of Standards and Technology, Standard Reference Data Program, Gaithersburg. Gaithersburg; 2018. Available from: https://www.nist.gov/srd/refprop
13. Kulhánek M, Dostál V. Thermodynamic Analysis and Comparison of Supercritical Carbon Dioxide Cycles. 2011;2–8. Available from: http://www.sco2powercyclesymposium.org/resource_center/system_concepts/thermodynamic-analysis-and-comparison-of-supercritical-carbon-dioxide-cycles
14. Wang K, Li M -j., Guo J-Q, Li P, Liu Z. A Systematic Comparison of Different S-CO_2 Brayton Cycle Layouts Based on Multi-Objective Optimization for Applications in Solar Power Tower Plants. Appl Energy. 2018;212(August 2017):109–21. Available from: https://doi.org/10.1016/j.apenergy.2017.12.031
15. Rowan TH. Thesis: Functional Stability Analysis of Numerical Algorithms SUBPLEX. Unpublished Dissertation. 1990. Available from: http://citeseerx.ist.psu.edu/viewdoc/summary?doi=10.1.1.31.5708
16. Powell MJD. The NEWUOA Software for Unconstrained Optimization without Derivatives. 2006;255–97. Available from: http://link.springer.com/10.1007/0-387-30065-1_16
17. Powell M. The BOBYQA Algorithm for Bound Constrained Optimization without Derivatives. NAREP 2009;39. Available from: http://www6.cityu.edu.hk/rcms/publications/preprint26.pdf